Journal of Engineering Physics and Thermophysics, Vol. 70, No. 6, 1997

MODELING OF ION-IMPLANTED ARSENIC DIFFUSION IN A POLYSILICON-SILICON SYSTEM

O. I. Velichko, F. F. Komarov, N. M. Lukanov, A. N. Muchinskii, N. L. Prokhorenko, and V. A. Tsurko

UDC 681.3+519.6

A model of transfer processes of impurity atoms in a polysilicon-silicon system which describes the segregation of the impurity at the phase boundary is constructed. An algorithm is developed and numerical calculations are made for arsenic diffusion with allowance for a nonuniform defect distribution at the phase boundary.

1. Introduction. In modern technologies for fabrication of silicon integrated circuits ion-implanted polysilicon Si^* layers are used as a source for diffusion of impurity atoms. This allows the creation of highly doped layers with few lattice defects and shallow *pn* junctions. A small number of defects in the doped region is achieved because the latter is formed as a result of thermal diffusion of the impurity and the radiation disturbances induced by ion implantation remain in the Si^* layer. On the other hand, the presence of a polysilicon layer substantially changes the character of thermal diffusion, providing, for instance, segregation of impurity atoms at the Si^*-Si interface [1].

Moreover, the diffusion process in polysilicon considerably differs from that in a single crystal, due to the Si^* structure, which consists of randomly oriented crystal grains and an intergrain amorphous substance. In the course of thermal annealing the characteristic grain size increases, which allows their ordering with the formation of "columns" oriented from the substrate to the layer surface. The above circumstances have necessitated the development of a diffusion model of impurity atoms in the Si^*-Si system and of software for modeling of the processes under consideration.

2. Model. The existing diffusion models deal with diffusion both in a grain and at the integrain boundary [2], and take into account the influence of the growth rate of grains and impurity accumulation at the Si^*-Si interface [3, 4]. It is assumed that at the polysilicon-silicon phase boundary two thin layers exist that considerably differ in their properties from the substance in the interior. Firstly, a layer of amorphous silicon, similar in properties to the grain boundary, is adjacent to the polysilicon. Its thickness l_a, which is about the thickness of the grain boundary l_{boun}, is 0.5 ... 1.5 nm. Secondly, with any method of polysilicon deposition onto silicon a quasi-oxide SiO_x layer is formed between them where $1.6 \leq x \leq 1.8$. Its thickness is from 0.5 to 1.0 nm. In [3, 4] it is assumed that due to segregation a considerable part of the total amount of the impurity (several percent in the case of arsenic diffusion) is accumulated in the first layer. This assumption is hardly probable, because the thickness of the amorphous layer is very small. Moreover, experimental data unambiguously indicate that the region where impurity segregation occurs extends for ≈ 0.03 μm on both sides of the Si^*-Si interface, i.e., by a distance considerably larger than l_a [1].

Our experiments concerned with ion-implanted arsenic redistribution in the Si^*-Si system under short-time thermal annealing conditions confirm the data of [1]. Representative results of these experiments are shown in Fig. 1. A polysilicon 0.087 μm-thick layer was grown on KEF-4.5 silicon substrates and 50 keV arsenic ions were

Belarusian State University, Minsk; Scientific-Production Complex "Technological Center," Moscow; Belarusian State University of Information Science and Radioelectronics, Minsk; Institute of Mathematics of the National Academy of Sciences of Belarus; Institute of Technical Cybernetics of the National Academy of Sciences of Belarus, Minsk. Translated from Inzhenerno-Fisicheskii Zhurnal, Vol. 70, No. 6, pp. 1025-1032, November-December, 1997. Original article submitted June 13, 1996.

 1062-0125/97/7006-0988$18.00

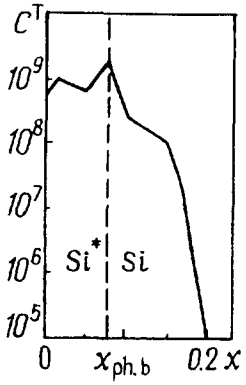

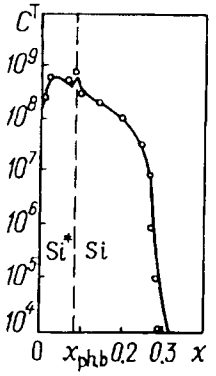

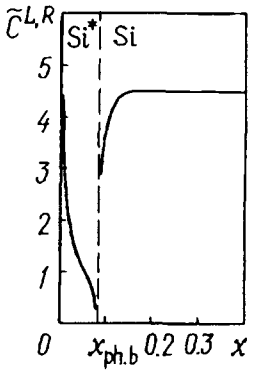

Fig. 1. Atomic distribution of arsenic after annealing at 950°C. C^T, μm^{-3}; x, μm.

Fig. 2. Calculated atomic distribution of arsenic after annealing at 1000°C (dots, measured total concentration values).

Fig. 3. Calculated defect distribution in the polysilicon-silicon system. $\tilde{C}^{L,R}$, rel. units.

implanted at a dose of 1500 $\mu C/cm^2$. Heat treatment was accomplished for 10 min at 950°C. To prevent impurity evaporation, the structure was passivated by a SiO_2 layer. The total concentration of impurity atoms was measured by the SIMS method. As seen in Fig. 1, the segregation region of the impurity extends by ≈ 0.015 μm on both sides of the phase boundary.

We construct a model of transfer processes of impurity atoms to describe adequately the impurity segregation near the Si*–Si interface. For this, we employ the results of numerical calculations of ion-implanted arsenic redistribution from [5]. As follows from [5], the impurity segregation in a near-surface region of the above dimensions can be described under the assumption that in this region a nonuniform distribution of point defects responsible for transfer of impurity atoms exists due to defect absorption by the semiconductor surface. Apparently, such a mechanism of segregation of impurity atoms is the best for describing the effects at the Si*–Si interface, since the polysilicon layer is an effective sink for inherent point defects existing in the monocrystalline silicon.

Without loss of generality, we assume that the transfer of impurity atoms in silicon is accomplished via defects of the same kind, namely, either vacancies or inherent interstitial atoms. Then impurity diffusion in silicon can be described by the equation [5, 6]

$$C_t^T = \nabla [D(\chi) \nabla (\tilde{C}C) + D(\chi) \tilde{C}C\nabla\chi/\chi], \quad (1)$$

where $C^T = C^A + C$, $\chi = [C - N + \sqrt{(C-N)^2 + 4n_i^2}]/(2n_i)$, $D(\chi) = D_i(1 + \beta_1\chi + \beta_2\chi^2)/(1 + \beta_1 + \beta_2)$, $\tilde{C} = C^\times/C_i^\times$.

Equation (1) is obtained under the assumption that the impurity transfer proceeds as a result of formation, migration and decay of the impurity atom – inherent point defect complexes. Assume that impurity transfer in polysilicon is accomplished by the same mechanism. Since within the scope of the present work we are interested in the macroscopic description of diffusion near the phase boundary we will not consider diffusion processes at the intergrain boundaries or in the grain interior separately but will employ the notion of the effective diffusion coefficient [7]. Based on this assumption, we describe diffusion in polysilicon by the equation

$$C_t^* = \nabla [D^* (\nabla (\tilde{C}^* C^*)], \quad \tilde{C}^* = C_{m^*}^*/C_{m^*i}^*. \quad (2)$$

Note, that Eq. (1) turns into (2) at $n_i >> C$. Therefore, mathematically the problem has been formulated as follows. The diffusion process is considered in the region $G = \{0 < x < l_x\}$, consisting of two phases, the phase boundary of which is specified by the coordinate $x_{ph.b}$. The diffusion process in each of the phases is described by Eq. (1), whose quantities have the superscripts L and R for the first (left-hand) and second (right-hand) phases, respectively. At the phase boundary these quantities are related by the expressions:

1) equality of the electrochemical potentials of impurity atoms μ on both sides of the phase boundary [8]

$$\mu^L|_{x=x_{ph.b}-0} = \mu^R|_{x=x_{ph.b}+0}; \tag{3}$$

2) the law of conservation of the amount of impurity atoms traversing the phase boundary

$$D^L(\chi^L)\,[\nabla(\tilde{C}^L C^L) + \tilde{C}^L C^L \nabla\chi^L/\chi^L]|_{x=x_{ph.b}-0} =$$

$$= D^R(\chi^R)\,[\nabla(\tilde{C}^R C^R) + \tilde{C}^R C^R \nabla\chi^R/\chi^R]|_{x=x_{ph.b}+0}. \tag{4}$$

Introducing the notion of the effective coefficient of impurity segregation k^s, condition (3) can be represented as

$$\left.\frac{C^{TR}}{C^{TL}}\right|_{x=x_{ph.b}} = k^s, \tag{5}$$

and the condition on the left-hand phase surface as

$$W_1 D^L(\chi^L)\,[\nabla(\tilde{C}^L C^L) + \tilde{C}^L C^L \nabla\chi^L/\chi^L] + W_2 C^L = W_3. \tag{6}$$

It is seen from (6) that depending on the parameters W_i, $i = 1, 2, 3$ we can specify conditions of the first ($W_1 = 0$, $W_2 \neq 0$, $W_3 \neq 0$), second ($W_1 \neq 0$, $W_2 = 0$) and third ($W_1 \neq 0$, $W_2 \neq 0$) kinds.

The boundary condition in the interior of the semiconductor volume can be represented as one of the first kind

$$C^R(l_x) = C_b. \tag{7}$$

and the initial condition for both phases as

$$C^T(x, 0) = C_0^T(x), \tag{8}$$

where the function $C_0^T(x)$ in the case of doping by ion implantation represents a Gaussian or, more accurately, a Pearson-IV distribution with the parameters determined from tables [9], depending on the kind of ions, energy, and implantation dose.

3. Equation of Defect Diffusion. To solve Eqs. (1) and (2) numerically, it is necessary to know the distribution of defects responsible for impurity diffusion in silicon and polysilicon. Therefore, these equations must be solved simultaneously with the diffusion equations of the corresponding defects. However, the characteristic feature of Eq. (1) is the presence of a concentration of defects in the neutral charged state in it, i.e., defects which are not affected by the internal electric field. The diffusion equation for such defects can be represented in the form [10]:

$$\tilde{C}_{xx} - \tilde{C}/l^2 + \tilde{C}_g/l^2 = 0, \quad l = \sqrt{d\tau}, \quad \tilde{C}_g = (g/g_i)/(\tau/\tau_i). \tag{9}$$

Defect diffusion equation (9) does not contain a drift term and in the case of defect generation or absorption at the phase boundaries allows an analytical solution. For polysilicon, for the first-kind boundary conditions, it has the form

$$\tilde{C}^L = \hat{C}_g^L + A_1^L \exp(-x/l^L) + A_2^L \exp(x/l^L), \tag{10}$$

where

$$A_1^L = \frac{\tilde{C}_s^L \exp(x_{ph.b}/l^L) - \tilde{C}_p^L + \tilde{C}_g^L [1 - \exp(x_{ph.b}/l^L)]}{\exp(x_{ph.b}/l^L) - \exp(-x_{ph.b}/l^L)},$$

$$A_2^L = \frac{\tilde{C}_{ph.b}^L - \tilde{C}_s^L \exp(-x_{ph.b}/l^L) - \tilde{C}_g^L [1 - \exp(-x_{ph.b}/l^L)]}{\exp(x_{ph.b}/l^L) - \exp(-x_{ph.b}/l^L)},$$

A similar solution for silicon has the form

$$\tilde{C}^R = \tilde{C}_l^R + A_1^R \exp(-x/l^R), \tag{11}$$

where

$$A_1^R = (\tilde{C}_{ph.b}^R - \tilde{C}_l^R) \exp(x_{ph.b}/l^R).$$

Substitution of analytical solutions (10), (11) into Eq. (1) makes it possible to solve only diffusion equation (1) of impurity in polysilicon and silicon layers instead of solving numerically a system of the diffusion equations for impurity atoms and intrinsic point defects.

4. Calculation Scheme. Mathematically, the diffusion process considered is described by a quasilinear parabolic equation in a region consisting of two phases at whose boundary the solution and the coefficients undergo a discontinuity. To solve this equation, we employ the method of finite differences [11]. Conservative difference schemes are built using the integro-interpolation technique [12]. Due to the nonclassical statement of the problem – solution discontinuity – the suggested difference schemes are inhomogeneous. Because of the algorithmic requirement of coincidence of the discontinuity point with a network node, we have used nonuniform space steps [13, 14]. The use of weights allows application of various classes of schemes [11]. To seek a solution of the system of nonlinear algebraic equations, use is made of iteration methods [15].

We reduce the diffusion equations to a form convenient for constructing a calculation scheme. From the essence of the problem statement, $C^T = C^T(C)$. Note also that $\chi = \chi(C)$ and, consequently, $D(\chi) = D(\chi(C)) = \tilde{D}(C)$. Let

$$D_1(C) = \tilde{D}(C), \quad D_2(C) = D_1(C)\,\tilde{C}C\,\frac{\partial \chi(C)}{\partial C}/\chi(C).$$

Then the diffusion model can be represented as

$$\frac{\partial C^{T\eta}(C^\eta)}{\partial t} = \frac{\partial}{\partial x}\left(D_1^\eta(C^\eta)\frac{\partial}{\partial x}(\tilde{C}^\eta C^\eta) + D_2^\eta(C^\eta)\frac{\partial C^\eta}{\partial x}\right), \quad x \in G, \quad x \neq x_{ph.b}, \quad 0 \le t \le T, \tag{12}$$

$$\left.\frac{C^{TR}(C^R)}{C^{TL}(C^L)}\right|_{x=x_{ph.b}} = k^s, \tag{13}$$

$$\left. D_1^L(C^L)\frac{\partial}{\partial x}(\tilde{C}^L C^L) + D_2^L(C^L)\frac{\partial C^L}{\partial x}\right|_{x=x_{ph.b}-0} =$$

$$= \left. D_1^R(C^R)\frac{\partial}{\partial x}(\tilde{C}^R C^R) + D_2^R(C^R)\frac{\partial C^R}{\partial x}\right|_{x=x_{ph.b}+0}, \tag{14}$$

$$W_1\left[D_1^L(C^L)\frac{\partial}{\partial x}(\tilde{C}^L C^L) + D_2^L(C^L)\frac{\partial C^L}{\partial x}\right] + W_2 C^L = W_3, \quad x = 0, \tag{15}$$

$$C^R = C_b\,,\quad x = l_x\,, \tag{16}$$

$$C^T(x, 0) = C_0^T(x)\,,\quad x \in G\,, \tag{17}$$

where $\eta = L$ at $x < x_{ph.b}$; $\eta = R$ at $x > x_{ph.b}$.

In the modeling region G we introduce a nonuniform network:

$$\hat{\bar{\Omega}}_h = \left\{x_i\,,\ i = 0, 1, ..., N\,,\ x_0 = 0\,,\ x_N = l_x\,,\ h_i = x_i - x_{i-1}\right\}.$$

The phase boundary coordinate $x_{ph.b}$ of the two phases is known; therefore. a nonuniform network can be always chosen such that the point $x_{ph.b}$ is its node.

The time network is also made nonuniform with a monotone increasing step τ_j

$$\hat{\bar{\Omega}}_\tau = \left\{t_j\,,\ j = 0, 1, ..., j_0\,,\ t_0 = 0\,,\ t_{j0} = T\,,\ \tau_j = t_j - t_{j-1}\right\}.$$

Write a balance equation for Eq. (12) in a rectangle $x_{i-1/2} \le x \le x_{i+1/2}$, $t_j \le t \le t_{j+1}$, $x_{i-1/2} = x_i - 0.5h_i$, $x_{i+1/2} = x_i + 0.5h_{i+1}$, $x_i \ne x_{ph.b}$

$$\int_{x_{i-1/2}}^{x_{i+1/2}} [C^{T\eta}(C^\eta)|_{t=t_{j+1}} - C^{T\eta}(C^\eta)|_{t=t_j}]\,dx = \int_{t_j}^{t_{j+1}} [\omega(x_{i+1/2}, t) - \omega(x_{i-1/2}, t)]\,dt\,, \tag{18}$$

where

$$\omega(x, t) = D_1^\eta(C^\eta)\frac{\partial}{\partial x}(\tilde{C}^\eta C^\eta) + D_2^\eta(C^\eta)\frac{\partial C^\eta}{\partial x}.$$

Next we approximate the integrals and derivatives entering the balance equation:

$$\int_{x_{i-1/2}}^{x_{i+1/2}} C^{T\eta}(C^\eta)\,dx \sim 0.5(h_i + h_{i+1})\,C^{T\eta}(C^\eta)|_{x=x_i}\,,$$

$$\omega_{i-1/2} \sim a_1^\eta(C_i^\eta)(\tilde{C}^\eta C^\eta)_{\bar{x},i} + a_2^\eta(C_i^\eta)\,C_{\bar{x},i}^\eta\,,$$

$$\frac{1}{\tau_{j+1}}\int_{t_j}^{t_{j+1}} \omega(x_{i-1/2}, t)\,dt \sim \sigma\omega_{i-1/2}^{j+1} + (1 - \sigma)\,\omega_{i-1/2}^{j}\,,$$

where $\sim$ is the approximation sign; σ, $0 \le \sigma \le 1$ is a numerical parameter. The coefficients a_1^η, a_2^η are expressed in terms of $D_1^\eta(C^\eta)$, $D_2^\eta(C^\eta)$ with the aid of model functionals [11].

After introducing the obtained expressions into (18) and substituting y for C we arrive at a difference scheme for the network function $y(x_i, t_j)$:

$$\frac{C^{T\eta}(\hat{y}^\eta) - C^{T\eta}(y^\eta)}{\tau_{j+1}} = \Lambda(\sigma\hat{y}^\eta + (1 - \sigma)\,y^\eta)\,,\quad x \in \hat{\bar{\Omega}}_h\,,\ x \ne x_{ph.b}\,,\ 0 \le t < T\,. \tag{19}$$

Here

$$\Lambda y^\eta = (a_1^\eta(y^\eta)(\tilde{C}^\eta y^\eta)_{\bar{x}})_{\hat{x}} + (a_2^\eta(y^\eta)\,y_{\bar{x}}^\eta)_{\hat{x}}.$$

Now we supplement Eq. (19) with additional conditions by approximating matching relations (13), (14), boundary and initial data (15)-(17) with the following expressions:

$$\frac{C^{TR}(\hat{y}^R)}{C^{TL}(\hat{y}^L)} f = k^s, \tag{20}$$

$$\sigma\omega^L(\hat{y}^L) + (1-\sigma)\,\omega^L(y^L) + 0.5h_{N_{ph.b}}/\tau_{j+1}\,[C^{TL}(\hat{y}^L_{N_{ph.b}}) - C^{TL}(\hat{y}^L_{N_{ph.b}})] =$$

$$\sigma\omega^R(\hat{y}^R) + (1-\sigma)\,\omega^R(y^R) - 0.5h_{N_{ph.b}+1}/\tau_{j+1}\,[C^{TR}(\hat{y}^R_{N_{ph.b}}) - C^{TR}(y^R_{N_{ph.b}})], \tag{21}$$

$$W_1\,[\sigma\omega^L_{boun}(\hat{y}^L_0) + (1-\sigma)\,\omega^L_{boun}(y^L_0)] + W_2\,[\sigma\hat{y}^L_0 + (1-\sigma)\,y^L_0] =$$

$$= W_3 + 0.5h_1 W_1/\tau_{j+1}\,[C^{TL}(\hat{y}^L_0) - C^{TL}(y^L_0)], \tag{22}$$

$$y^R = C_b, \quad x = l_x, \quad 0 < t \le T, \tag{23}$$

$$y(x, 0) = C_0^T(x), \quad x \in \hat{\Omega}_h, \tag{24}$$

where

$$\omega^L(y^L) = a_1^L(y^L)(\tilde{C}^L y^L)_{\bar{x}} + a_2^L(y^L)\,y^L_{\bar{x}},$$

$$\omega^R(y^R) = a_1^R(y^R)(\tilde{C}^R y^R)_x + a_2^R(y^R)\,y^R_x, \tag{25}$$

$$\omega^L_{boun}(y^L) = a_1^L(y^L_1)(\tilde{C}^L y^L)_{x,0} + a_2^L(y^L_0)\,y^L_{x,0}.$$

To determine $\hat{y} = y^{j+1} = (\hat{y}^L, \hat{y}^R)$ on a new layer, we use the system of nonlinear Eqs. (19)-(24). To solve the latter, we employ the following iteration technique:

$$C^{T\eta}(\overset{k}{y}{}^{\eta}) + (C^{T\eta}(\overset{k}{y}{}^{\eta}))'(\overset{k+1}{y}{}^{\eta} - \overset{k}{y}{}^{\eta}) - \tau_{j+1}\,\sigma\Lambda(\overset{k+1}{y}) = C^{T\eta}(y^{\eta}) + \tau_{j+1}(1-\sigma)\,\Lambda y, \tag{26}$$

$$\frac{\overset{k+1}{y^R_{k+1}}}{\overset{k+1}{y^L}} = k^s \frac{F^L(\overset{k}{y^L})}{F^R(\overset{k}{y^R})}, \tag{27}$$

$$\sigma\omega^L(\overset{k+1}{y}{}^L_{N_{ph.b}}) + (1-\sigma)\,\omega^L(y^L_{N_{ph.b}}) + 0.5h_{N_{ph.b}}/\tau_{j+1}\,[C^{TL}(\overset{k}{y}{}^L_{N_{ph.b}}) +$$

$$+ (C^{TL}(\overset{k}{y}{}^L_{N_{ph.b}}))'(\overset{k+1}{y}{}^L_{N_{ph.b}} - \overset{k}{y}{}^L_{N_{ph.b}}) - C^{TL}(y^L_{N_{ph.b}})] =$$

$$= \sigma\omega^R(\overset{k+1}{y}{}^R_{N_{ph.b}}) + (1-\sigma)\,\omega^R(y^R_{N_{ph.b}}) + 0.5h_{N_{ph.b}+1}/\tau_{j+1}\,[C^{TR}(\overset{k}{y}{}^R_{N_{ph.b}}) +$$

$$+ (C^{TR}(\overset{k}{y}{}^R_{N_{ph.b}}))'(\overset{k+1}{y}{}^R_{N_{ph.b}} - \overset{k}{y}{}^R_{N_{ph.b}}) - C^{TR}(y^R_{N_{ph.b}})], \tag{28}$$

$$W_1 [\sigma \omega^L_{\text{boun}} (\overset{k+1}{y^L_1}) + (1-\sigma)\, \omega^L_{\text{boun}} (\overset{L}{y_1})] + W_2 [\sigma \overset{k+1}{y^L_0} + (1-\sigma)\, \overset{L}{y_0}] = W_3 +$$

$$+ 0.5 h_1 W_1/\tau_{j+1} [C^{TL} (\overset{k}{y^L_0}) + (C^{TL} (\overset{k}{y^L_0}))' (\overset{k+1}{y^L_0} - \overset{k}{y^L_0}) - (C^{TL} (\overset{L}{y_0})), \tag{29}$$

$$\overset{k+1}{y^R_N} = C_b . \tag{30}$$

Here

$$\Lambda (\overset{k+1}{y}) = (a^\eta_1 (\overset{k}{y^\eta}) (\tilde{C}^\eta \overset{k+1}{y^\eta})_{\bar{x}})_{\hat{x}} + (a^\eta_2 (\overset{k}{y^\eta}) (\overset{k+1}{y^\eta_{\bar{x}}}))_{\hat{x}} .$$

Similarly, difference approximations (25) are calculated: $\omega^L (\overset{k+1}{y^L})$, $\omega^R (\overset{k+1}{y^R})$ and $\omega^L_{\text{boun}} (\overset{k+1}{y^L_1})$.

The functions F^L, F^R are determined from the relations

$$C^{TL} (C^L) = C^L F^L (C^L), \quad C^{TR} (C^R) = C^R F^R (C^R) .$$

As the initial iteration, we take the function $y = (y^L, y^R)$ of the preceding time step, $\overset{0}{y} = y^j$. Difference equations (26), (28) are reduced to the form

$$A_i \overset{k+1}{y^L_{i-1}} - C_i \overset{k+1}{y^L_i} + B_i \overset{k+1}{y^L_{i+1}} = -F_i , \quad i = 1, 2, \ldots, N_{\text{ph.b}} - 1 ,$$

$$A_i \overset{k+1}{y^L_{i-1}} - C_i (\overset{k+1}{y^L_i} + \overset{k+1}{y^R_i}) + B_i \overset{k+1}{y^R_{i+1}} = -F_i , \quad i = N_{\text{ph.b}} , \tag{31}$$

$$A_i \overset{k+1}{y^R_{i-1}} - C_i \overset{k+1}{y^R_i} + B_i \overset{k+1}{y^R_{i+1}} = -F_i , \quad i = N_{\text{ph.b}} + 1 , N_{\text{ph.b}} + 2 , \ldots, N .$$

Taking into account (27) and supplementing (31) with the conditions at the boundaries (29), (30), we obtain a system of three-point linear algebraic equations for $\overset{k+1}{y_i}$, $i = 0, 1 \ldots, N$ which is solved by the factorization method [11, 15]. Iteration is performed until the condition

$$| \overset{k+1}{y_i} - \overset{k}{y_i} | \le \varepsilon_1 | \overset{k}{y_i} | + \varepsilon_2 , \quad i = 0, 1, \ldots, N$$

is fulfilled.

Some aspects of the suggested numerical method were checked on model problems, whose solution can be estimated with sufficient reliability. Variation of time and space steps, weights, iteration parameters makes it possible to control calculations.

An additional tool for calculation control is checking the fulfillment of the relation

$$\int_0^{x_{\text{ph.b}}} C^{TL}\, dx + \int_{x_{\text{ph.b}}}^{l_x} C^{TR}\, dx = \text{const}$$

in the case when an impurity flow across the surface is absent. For the problem considered below the change in the integral did not exceed 1.5%.

5. Results of Numerical Calculations. Representative results for the redistribution of ion-implanted arsenic in the polysilicon-silicon system are shown in Fig. 2. For experiments, use was made of KÉF-4.5 substrates on which a 0.087 μm thick polysilicon layer was grown and implantation of 50 keV arsenic ions at a dose of 1500

$\mu C/cm^2$ was accomplished. Heat treatment was conducted at 1000°C for 10 min. To prevent impurity evaporation, the structure was passivated by a SiO_2 layer.

In calculations, we used the following values of quantities characterizing the initial impurity distribution and the transfer of impurity atoms: $R_p = 0.038$ μm; $\Delta R_p = 0.014$ μm; $S_k = 0.45$ [9]; $C_m^T = 2.69 \cdot 10^9$ m; $D^* = D^L = 2.5 \cdot 10^{-6}$ μm^2/sec [16]; $D_i = D_i^R = 1.69 \cdot 10^{-7}$ μm^2/sec [16]; $n_i = n_i^R = 8.85 \cdot 10^6$ μm^{-3}; $\beta_1 = \beta_1^R = 7.3$; $\beta_2 = \beta_2^R = 0.13$.

To determine β_1 and β_2, we used data on the concentration-dependent diffusion coefficient of arsenic [17]. For this purpose, they were represented as a dependence on the electron concentration but not on the total concentration of the impurity. The parameters β_1 and β_2 were determined from the condition of the best agreement of the calculated concentration dependence of the diffusion coefficient $D(\chi)$ and the experimental data. The concentration dependence of the diffusion coefficient was recalculated using the empirical formula for the total impurity concentration deried in [18]:

$$C^T = C^A + C = \beta^A C^4 + C,$$

where $\beta^A = 1.00 \cdot 10^{-25}$ μm^9 at 1000°C. This formula was also employed to describe the cluster formation of arsenic in silicon by solving impurity diffusion equation (1) numerically.

To describe the states of the defect subsystem, we used the following set of parameters: in polysilicon – $l^* = l^L = 0.015$ μm; $\tilde{C}_s^* = \tilde{C}_s^L = 5.0$, $\tilde{C}_{ph.b}^* = \tilde{C}_{ph.b}^L = 0.05$, $\tilde{C}_g^* = 1.0$; in silicon – $l = l^R = 0.015$ μm; $\tilde{C}_{ph.b}^* = \tilde{C}_{ph.b}^R = 3.0$; $\tilde{C}_g^* = 4.5$.

The calculated defect-distributions in silicon and polysilicon used in modeling the process of arsenic redistribution (see Fig. 2) are given in Fig. 3 (for the neutral charged state).

As is seen from Fig. 2, the calculation results are in fair agreement with the experimental data. Moreover, the suggested model adequately describes the phenomenon of "ascending" diffusion on near-surface regions on both sides of the Si*–Si phase boundary.

Good agreement with experiment is observed both in silicon and polysilicon, though we introduced the notion of the effective diffusion coefficient to describe the transfer processes in polysilicon. The agreement with experiment allows one to use this model as a basis in development of a modeling program for the technology of fabrication of bipolar transistors of large-scale silicon integrated circuits by ion implantation in polysilicon layers. Moreover, this model and developed software can be used to describe other transfer processes at the phase boundaries of two phases, for instance, to model the process of superlattice disordering in complex semiconductors [19].

NOTATION

C^T, total atomic concentration of the impurity; C^A and C, concentrations of the impurity atoms bound into clusters and of the substitutional atoms, respectively; χ, electron (hole) concentration reduced to n_i in the case of doping by an n-type (p-type) impurity; n_i, concentration of intrinsic charge carriers; N, concentration of the impurity with opposite type of conductivity; C^*, impurity concentration in polysilicon; C_b, background volume atomic concentration of the impurity in the semiconductor; l_x, coordinate of the right-hand boundary of the modeling region; $D(\chi)$, effective diffusion coefficient of the impurity in silicon; D^*, effective diffusion coefficient of the impurity in polysilicon; D_i, self-diffusion coefficient of the impurity atoms; β_1 and β_2, empirical constants describing relative contribution to the diffusion of singly and doubly charged defects as compared to the contribution of defects in the neutral charged state; $C_m^\times$, concentration of intrinsic point defects of species m in silicon in the neutral charged state; C_i, thermal-equilibrium concentration of this species; $C_{m^*}^*$, concentration of point defects of species m^* in polysilicon responsible for transfer of impurity atoms; $C_{m^*i}^*$, thermal-equilibrium concentration of these defects; d and τ, effective diffusion coefficient and mean lifetime of defects, respectively; g, generation rate of these defects per unit volume of the substance; g_i and τ_i thermal-equilibrium values of g and τ, respectively; R_p and ΔR_p, mean projective range of the ion path and the path straggling, respectively; S_k, asymmetry of the impurity

distribution profile; C_m^T, impurity concentration at the maximum of the Gauss distribution; l, mean diffusion path length of defects; $\tilde{C}_s^L$ and $\tilde{C}_{ph.b}^L$, defect concentration in polysilicon on the surface and at the phase boundary, respectively, normalized to thermal-equilibrium defect concentration $C_{m^*i}^*$ in polysilicon; l^L, mean path length of defects in polysilicon; $\tilde{C}_{ph.b}^R$ and $\tilde{C}_l^R$, concentration of neutral point defects in silicon at the phase boundary and at $x = l_x$, respectively, normalized to the thermal-equilibrium concentration of these defects $C_i^\times$; T, heat treatment time; t, current time. Subscripts: ph. b, phase boundary; s,surface. Superscript: s, segregation.

REFERENCES

1. H. Ryssel, H. Iberl, M. Bleier, G. Prinke, K. Haberger, and H. Kranz, J. Appl. Phys., **24**, No. 3, 197-200 (1981).
2. B. J. Mulvaney, M. B. Richardson, and T. L. Grandle, IEEE Trans., CAD-8, No. 4, 336-348 (1989).
3. A. G. O'Neil, O. Hill, J. King, et al., J. Appl. Phys., **64**, No. 1, 167-174 (1988).
4. A. D. Sadovnikov and A. V. Chernyaev, Mat. Model, **2**, No. 8, 60-69 (1990).
5. V. A. Labunov and O. I. Velichko, Inzh.-Fiz. Zh., 57, No. 5, 805-810 (1989).
6. O. I. Velichko, Radiotekhnika i Elektronika, Republican Interdepartmental Correlated Works, Minsk, Issue 14 (1985), pp. 91-94.
7. C. P. Ho, J. D. Plummer, S. E. Hansen, and R. W. Dutton, IEEE Trans., **ED-30**, No. 11, 1438-1453 (1983).
8. V. N. Chebotin, Physical Chemistry of Solids [in Russian], Moscow (1982).
9. A. F. Burenkov, F. F. Komarov, M. A. Kumakhov, and M. M. Temkin, Space Distributions of the Energy Released in a Cascade of Atomic Collisions in Solids [in Russian], Moscow (1985).
10. V. A. Labunov, O. I. Velichko, and S. K. Fedoruk, Inzh.-Fiz. Zh., 67, No. 5-6, 433-436 (1994).
11. A. A. Samarskii, The Theory of Difference Schemes [in Russian], Moscow (1989).
12. A. N. Tikhonov and A. A. Samarskii, Zh. Vych. Mat. i Mat. Fiz., **1**, No. 1, 5-63 (1961).
13. A. N. Tikhonov and A. A. Samarskii, Zh. Vych. Mat. i Mat. Fiz., 2, No. 5, 812-832 (1962).
14. A. A. Samarskii, Zh. Vych. Mat. i Mat. Fiz., 3, No. 2, 266-298 (1963).
15. A. A. Samarskii and E. S. Nikolaev, Methods for Solution of Net Equations [in Russian], Moscow (1978).
16. J. Tsai, The LSIC Technology [in Russian], Vol. 1, Moscow (1986), pp. 227-291.
17. R. B. Fair and J. C. C. Tsai, J. Electrochem. Soc.: Solid-State Sci. and Technol., **122**, No. 12, 1689-1696 (1975).
18. K. Tsukamoto, Yo. Akasaka, and K. Kijima, Jap. J. Appl. Phys., **19**, No. 1, 87-95 (1980).
19. D. G. Deppe and N. Holonyak, Jr., J. Appl. Phys., **64**, No. 12, R93-R113 (1988).